NRL Report 6768

The Plate Materials of the Lead-Acid Cell

Part 4 - Anodic Oxidation of Three Representative Oxides

JEANNE BURBANK

Electrochemistry Branch
Chemistry Division

September 25, 1968

NAVAL RESEARCH LABORATORY
Washington, D.C.

This document has been approved for public release and sale; its distribution is unlimited.

PREVIOUS REPORTS IN THE SERIES

"Part 1 – Anodic Oxidation of the Basic Sulfates of Lead," J. Burbank, NRL Report 6345, Nov. 1965

"Part 2 – Anodic Oxidation of $PbSO_4$, Pb_3O_4, $2PbCO_3 \cdot Pb(HO)_2$, and Orthorhombic PbO," J. Burbank, NRL Report 6450, Oct 1966

"Part 3 – Anodic Oxidation of Tetragonal PbO," J. Burbank, NRL Report 6613, Dec. 1967

CONTENTS

Abstract	ii
Problem Status	ii
Authorization	ii
INTRODUCTION	1
MATERIALS AND METHODS	1
RESULTS	4
ACKNOWLEDGMENT	11
REFERENCES	11

ABSTRACT

Three representative lead oxides, designated A, C, and H, for storage-battery fabrication were mixed with water and H_2SO_4 to paste consistency. Each of these was hand pasted into antimonial and pure-lead circular grids of standard SLI thickness. The plates were cured according to common practice for each oxide. The small circular plates were anodized in an electrolytic cell mounted directly on an x-ray machine, and the diffraction patterns were recorded at intervals throughout 72 hr of formation in 1.0585 sp gr H_2SO_4.

X-ray diffraction patterns from the unformed pastes showed the major component was tribasic lead sulfate in all three. The surfaces of plates made from oxides A and H were primarily basic lead carbonate (hydrocerussite), and the surfaces of plates made with oxide C were largely tribasic lead sulfate. Residual PbO and, in the case of oxide H, Pb_3O_4 also were detected. During the soaking period, normal $PbSO_4$ formed on the surfaces of all plates, rapidly eliminating any basic carbonate. During this period Pb_3O_4 in paste H became converted to PbO_2 and $PbSO_4$ causing a marked color change in this kind of plate. As oxidation progressed, dark brown to black βPbO_2 developed near the grid bars and spread gradually toward the pellet centers. Paste A formed at the edges and interior of the pellets but retained a surface coating of $PbSO_4$ at the pellet centers. Pastes C and H appeared essentially completely oxidized, paste C giving a very dark blackish plate, while paste H was lighter in color.

On completion of anodization, nominally 150% of the theoretical requirement on a weight basis, the plates were blotted and dried in air at room temperature. The formed paste was removed from the grids for electron-microscope examination by carbon replication. The PbO_2 had a range of morphologies, and the individual crystallites varied from about 0.5 μ to less than 0.1 μ. Some prismatic crystals with branching suggestive of multiple twinning were present in paste A and appeared less frequently in the other two pastes. Agglomerates, several microns in size, of prismatic crystallites were present in all pastes. Paste H gave rise to the largest individual crystallites which were about 0.5 μ in diameter. Oxide C resulted in remarkably uniform 0.1-μ crystallites arranged in spiraling layers terminating in one central individual crystallite, forming spheroidal agglomerates. Although not always clearly obvious in the electron micrographs, it is believed that the aggregates are compound spikes of dendritic growth covered with sessile crystallites of varied size and morphology.

PROBLEM STATUS

This report concludes one phase of the problem; work on other phases is continuing.

AUTHORIZATION

NRL Problem C05-14
Projects SF 013-06-03-4366 and RR 001-01-43-4755

Manuscript submitted July 2, 1968.

THE PLATE MATERIALS OF THE LEAD-ACID CELL

PART 4 - ANODIC OXIDATION OF THREE REPRESENTATIVE OXIDES

INTRODUCTION

Positive plate materials of the lead-acid cell have received intensive study in recent years because of the massive failure of nonantimonial submarine cells in which the positive active material suffered catastrophic softening early in life. It was shown that similar cells, pasted with identical materials but having antimonial lead grids, gave longer service life. The difference in performance was attributed to the difference in electron morphology of the PbO_2 crystals, which in the case of the antimonial cells remained characteristically prismatic and dendritic, while those in a softening paste were nondescript spheroids, readily detached from the plate on overcharge gassing. These results have led to a systematic examination of the electron morphology of PbO_2 crystals in the lead-acid cell. It has been indicated that the electron morphology is related to the materials originally present in the paste (1-6).

MATERIALS AND METHODS

Three representative commerical oxides for storage-battery fabrication were used in this study, designated as A, C, and H in Table 1. These are characterized in Tables 2 and 3, which show the particle-size ranges and spectrographic analyses.

Table 1
Description of Oxides A, C, and H

Oxide	Description	Specific Surface (m^2/g)	Median Particle Radius (μ)*
A	A milled, nonleady litharge having a mixed composition of orthorhombic and tetragonal PbO	0.18	3.9
C	A leady litharge containing 25% free lead produced by ball milling	0.97	1.8
H	A furnaced oxide containing 25% Pb_3O_4	0.28	2.15

*Equivalent spherical radius.

Pastes of each oxide, water, and H_2SO_4 were mixed in a laboratory dough-type mixe in 3-lb batches (Table 4). Each of the pastes was hand pasted into special grids, cured, and dried according to standard practice for each type of oxide. Plates containing pastes of oxides A and H were racked and placed in a steam-filled oven to set the paste, followe by drying at about 105°C. Plates containing paste C were flashed, rolled, stacked, and cured for 24 hr in an insulated box, followed by 40 hr in a closed oven at 40.9°C. Conventional square grids for use as counter electrodes were pasted and cured at the same time, with the same materials.

Table 2
Particle-Size Distribution of Oxides A, C, and H

Particle-Size Range* (μ)	Particle-Size Distribution (wt-%) of Three Oxides		
	A	C	H
0.0 - 0.015	0.03	0.9	0.02
0.015 - 0.03	0.05	1.2	0.06
0.03 - 0.06	0.14	2.2	0.22
0.06 - 0.125	0.38	4.2	0.7
0.125 - 0.25	1.0	6.5	1.8
0.25 - 0.5	2.0	10.0	4.7
0.5 - 1	5.4	12.0	11.5
1 - 2	13.0	15.0	28.0
2 - 4	39.0	15.0	34.0
4 - 8	20.0	14.0	16.3
8 - 16	14.5	12.5	2.57
16 - 32	4.1	5.8	0.13
32 - 64	0.4	0.7	—
plastic (< 0.5)	3.6	25	7.5
granular (> 0.5)	96.4	75	92.5

*Equivalent spherical radius.

Table 3
Spectrographic Analysis of Oxides A, C, and H

Element or Compound	Distribution of Element or Compound (wt-%) in Three Oxides		
	A	C	H
Ag	0.0005	0.00039	0.00039
Al_2O_3	0.00018	0.00005	0.00065
$BaSO_4$	<0.00020	<0.00020	0.00022
Bi	0.0026	0.017	0.020
CaO	0.00074	0.00020	0.0068
Cu	0.00034	0.00027	0.00048
Fe	0.00023	0.00009	0.0017
MgO	0.00053	0.00005	0.00084
Mn	Not detected	Not detected	0.00002
SiO_2	0.0020	0.00058	0.0074

Table 4
Pasting Data

Oxide	Initial Water (cc/lb)	H_2SO_4, 1.400 sp gr (cc/lb)	Final Water (cc/lb)	Paste Density (g/in^3)	Pasting Properties
A	50	40	None	65	Fair
C	50	40	None	65	Good
H	53	39	5	66	Good

The special and conventional square grids fabricated for this study were cast from pure lead and nominal 7% lead-antimony alloy. Spectrographic analyses of the grid metals are given in Table 5. The special grids were small circles with a 47-mm diameter designed to fit the electrolytic cell mounted directly on an x-ray goniometer, permitting registration of diffraction patterns during anodic treatment (7). Radiographs of each of the circular plates were made prior to any electrochemical treatment with a Faxitron 804 table-top radiographic system.

Table 5
Spectrographic Analyses of Grid Metals

Element	Grid Metals	
	Pure Lead (wt-%)	Antimonial Lead (wt-%)
Sb	Not detected	7.0
Sn	Not detected	0.3
As	Not detected	0.062
Bi	0.018	0.016
Cu	0.00015	0.0064
Fe	0.0017	0.00078
Mn	0.00002	0.00002
Mg	0.00014	0.00028
Si	0.00075	0.00044
Mo*	Not detected	Not detected
Cd	Not detected	Not detected
Ag	0.0014	0.0015
Ni	0.00005	0.00005
Ca	0.0004	0.0002

*Data given for elements from Mo to Ca are of lower precision.

The small disk plates were mounted in turn in the electrolytic cell, backed by a circle of pure lead to effect electrical contact, and rotated at 60 rpm throughout the anodization of about 72 hr, or less in certain instances (Table 6). A preliminary soak of 20 to 30 min was given in the electrolyte 1.0585-sp gr H_2SO_4. Anodic oxidation took place from one side only in the x-ray cell assembly, and the current density was approximately 4 ma/cm^2 on the submerged half of the electrode. Using Cu $K\alpha$ radiation, x-ray diffraction patterns were registered from the dry plate surfaces and from samples of paste removed from the grids, ground to pass type 120 sieve, mounted in the conventional manner for diffractometric registration. Following the soaking period, and at intervals throughout the anodic oxidation, diffraction patterns of the surfaces of the plates were recorded also. Positive plate polarization was followed continuously by means of a standard Hg/Hg_2SO_4 reference electrode.

On completion of anodization, usually about 150% of the theoretical requirement on a weight basis, the plates were blotted and dried in air at room temperature. The active

Table 6
Anodization Treatments

Oxide	Grid Metal	Average Plate Thickness (mm)	Dry Active Material Weight (g)	Theoretical Ampere-Hour	Actual Ampere-Hour	Percent
A	Pb-Sb	1.8288	7.6	1.79	1.165	65.08
		1.8288	6.3	1.49	2.252	151.15
		1.7018	6.4	1.51	2.304	128.72
	Pb	2.1082	8.2	1.94	3.024	155.9
C	Pb-Sb	2.1336	7.5	1.75	2.63	150.2
	Pb	2.1336	8.6	2.03	3.053	150.25
H	Pb-Sb	1.7018	7.0	1.65	2.52	152.7
	Pb	1.9304	8.7	2.05	3.024	147.51

material was removed from the grids for electron microscope examination by carbon replication and further x-ray diffraction study by the same methods used in the earlier studies (1-6). All electrochemical experiments were performed at room temperature, which varied from 20.0 to 25.2°C.

RESULTS

The radiographic examination of the cured plates showed that from a practical standpoint the grids were fairly well filled with paste and were free of large voids or skips. There were, however, hidden cracks in some pellets, and some areas of the grid bars were not in good intimate contact with the paste. A difference was observed between the radiographic density exhibited by the paste of oxide C and that of the other two oxides. It is seen in Fig. 1 that the paste containing oxide C is markedly more uniformly dense than that of oxide A, which was adopted as a standard for comparison of all plates. While it is true that the plates containing oxide C averaged thicker than the others (Table 6), there were variations among all specimens that eliminate thickness as the sole cause of this difference in radiographic density. Also, it may be observed from the figure that the plate of oxide A is distinctly more grossly porous than the paste resulting from oxide C. This was true of all specimens of pastes A and H when similarly compared with all those containing oxide C. Further, cross-pellet cracking was most prominent in oxide C as a general characteristic, as was poor contact with the grid bars.

From these observations it is concluded that paste C suffered greater shrinkage during curing than either paste A or H. Neglecting the fact that the curing reaction of oxide C must include the oxidation step of the free metallic lead particles present in this type of oxide and considering only the distribution of particle sizes in the original oxides (Table 2), it is not surprising that the oxide containing the lowest percentage of granular size particles would undergo the most pronounced shrinkage. The pasting properties (Table 4) of each of the oxides may be related to the relative amounts of granular- and plastic-size particles (Table 2). Oxide A had only 3.6% of plastic material and gave a paste described as "fair" in pasting quality. Oxides C and H had 25% and 7.5% plastic material, respectively, and both had good pasting properties. This suggests that 3.6% plastic material is too low to impart satisfactory workability to the mix, 7.5% is sufficient, and perhaps 25% is excessive, leading to the undesirable shrinkage cracking.

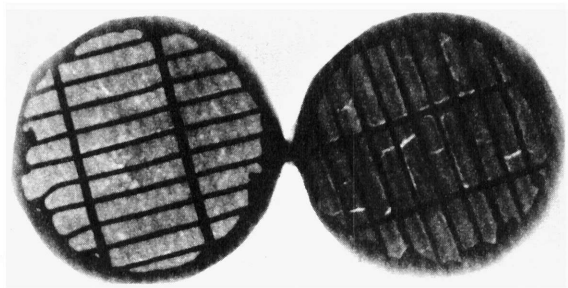

Fig. 1 - Representative macroradiographs of unoxidized, cured plates containing pastes from oxide A (left) and C (right). The dense packing of oxide C is shown by its greater opacity to x rays, giving a darker image than that of paste A. The distribution of macroporosity in paste A is shown by the fairly uniform mottling. Thin white lines are cracks, visible along some grid bars in paste A but larger and more extensive in paste C where shrinkage resulted in cross-pellet cracking as well as parting from the grid bars. Similar radiographs from plates containing paste H resembled the one shown for paste A.

Investigation of the rheological properties of these three representative oxides combined with simultaneous radiographic study of pasting and curing would be of interest. As a result, optimum workability could be realized, and pellet cracking and arcing along grid bars could be minimized and possibly eliminated.

All identifications of solid crystalline materials given in this report were made by x-ray diffraction analyses. Reference diffraction patterns are listed in Table 7 giving the card numbers in the standard file (8).

X-ray diffraction patterns from bulk specimens of the cured pastes showed the major component to be tribasic lead sulfate in all three. The surfaces of plates made with oxides A and H were primarily basic lead carbonate (hydrocerussite), and the surfaces of plates made with oxide C were largely tribasic lead sulfate. Residual PbO and, in the case of oxide H, Pb_3O_4 were also detected.

When plates containing oxides A and H came into contact with the dilute H_2SO_4 solution, the gassing of CO_2 was visible, and during the preliminary soaking period all traces of the superficial layers of basic lead carbonate were rapidly eliminated. Crystalline $PbSO_4$ formed on the surface of all three types of plate during the soaking period. At this same time, Pb_3O_4 in paste H was converted to PbO_2 and $PbSO_4$ and resulted in a marked purplish coloration in this kind of plate.

The plates were individually anodically oxidized; details of the anodizations are given in Table 6. The positive plate polarization during oxidation followed the expected pattern previously reported by Ikari, Yoshizawa, and Okada (12); one example is shown in Fig. 2. The actual values of the polarization will, of course, vary with the rate or current density, concentration of the electrolyte, and various IR losses in the system, such as plate thickness and compactness of the $PbSO_4$ coating on the outer surface of the plates.

Table 7
X-Ray Diffraction Patterns

Compound	ASTM (8) Card Number	Remarks
$PbSO_4$	5-0577	Excellent match is obtained for this material; on occasion the weak line at 5.38 is missing and with lesser amounts of $PbSO_4$ present only the strong lines are detected.
βPbO_2	8-185	Excellent match is obtained for this material with the exception of the line at 2.21, which did not appear in the electrochemical products of this study. There was some indication of preferred orientation in some of the electrodeposits, although not to a strong degree.
PbO (tetragonal)	5-0561	Excellent match is obtained for this material. On occasion, preferred orientation causes divergence from the standard intensities.
PbO	5-0570	Excellent match is obtained for this material.
Pb_3O_4	8-19	Excellent match is obtained for this material.
$Pb_3(CO_3)_2(OH)_2$	13-131	This reference card gives the best match for this material when observed as a reaction product on a surface; it arises from an oriented deposit with the basal planes lying in the surface. Because of the strong tendency for this material to form oriented deposits, the lattice parameters given on this card are in error. (Card 14-18 and Refs. 9 and 10.)
$3PbO \cdot PbSO_4 \cdot H_2O$	6-0282	This reference card gives a fairly good match for identification of this material, although weak lines are often missing and relative intensites may vary.
	6-0287	This reference card also gives a fairly good match for this material; however, the preparation contained some $4PbO \cdot PbSO_4$, and lines from this compound must be subtracted from the pattern. Bode and Voss (11) have given a pattern for this compound that compares favorably with the two given above. Comments: Identification of this material by x-ray diffraction in a mixture such as the battery paste is made on the basis of strong lines which fortunately are unique for this material.

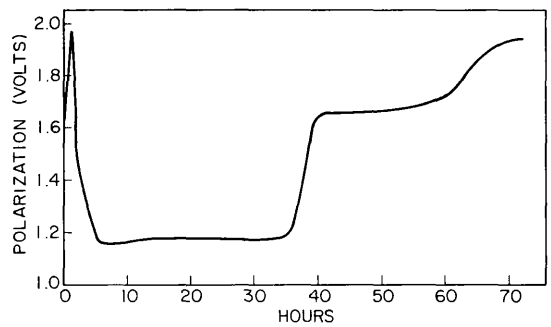

Fig. 2 - Plate polarization during anodic oxidation. The polarization is given relative to the standard Hg/Hg_2SO_4 reference electrode and is a typical example. Theoretically, if the process were 100% efficient, oxidation would have been complete at 48 hr at the constant current of approximately 4 ma/cm^2. The initial rise in polarization is attributed to an initial increase in resistance caused by continued deposition of $PbSO_4$ in the plate. This is followed by a lowering of resistance as the grid metal becomes covered with conducting PbO_2. When sufficient PbO_2 has been formed in the paste mass, between 36 and 40 hr in this case, the potential rises owing to the high oxygen overpotential on PbO_2 and ultimately climbs to the high terminal value when oxygen evolution becomes the major reaction during the final 10 hr of oxidation.

As the anodic oxidation progressed, dark brown to black βPbO_2 developed near the grid bars and spread gradually toward the pellet centers. Paste A became converted to PbO_2 at the edges and interior of the pellets but retained a surface coating of $PbSO_4$ at the pellet centers. Pastes C and H appeared essentially completely oxidized, paste C giving a very dark-blackish plate, while paste H was lighter in color. Figure 3 shows the general appearance of the plates at various stages of the work.

After formation, electron microscopy showed a range of morphologies with the individual crystallites varying from about 0.5 μ to less than 0.1 μ. Some prismatic crystals with branching suggestive of multiple twinning were present in paste A and appeared less frequently in the other two pastes. Agglomerates, up to several microns in size, of prismatic crystallites were present in all pastes. Paste H gave rise to the largest individual crystallites, which were about 0.5 μ in diameter. Oxide C resulted in many remarkably unifrom 0.1-μ crystallites arranged in spiraling layers terminated by one central individual crystallite and forming spheroidal agglomerates (Figs. 4-7). Although not always clearly apparent in the electron micrographs, it is believed that the aggregates are compound spikes of dendritic growth covered with sessile crystallites of varied size and morphology. It is possible that the agglomerates may arise from the coarse particles present in the original oxides.

Differences in PbO_2 morphology from the three different oxides were recognizable, and the photographs have been selected to illustrated these differences. Paste A appeared to give rise to true spherulites, paste C produced spheroidal agglomerates of small crystals from which emerged dendritic spikes of somewhat larger crystals, and paste H produced irregular-shaped clusters of even larger crystals. Because the largest individual

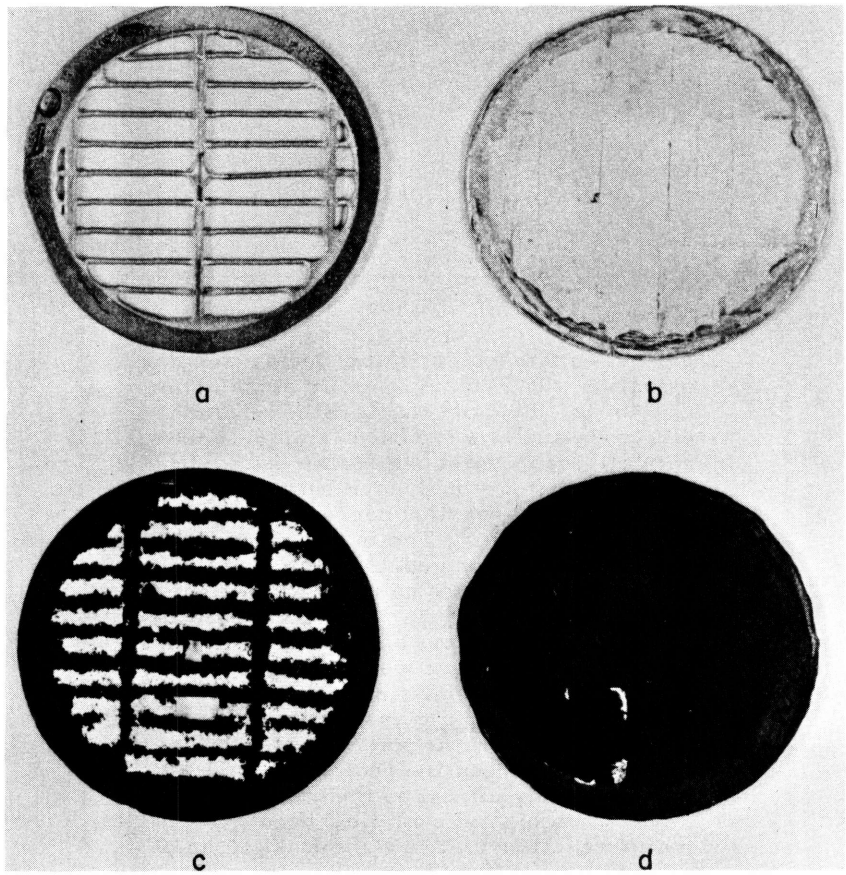

Fig. 3 - Small circular plates at various stages of the study: a. small grid prior to pasting, b. small plate after pasting and curing, c. small plate after partial anodization. Black β PbO_2 first appeared adjacent to the grid bars and gradually extended into the central pellet areas as anodization continued. The white areas were $PbSO_4$. In plates containing oxide A, a considerable residue of the white layer remained at the outer central surfaces of the pellets after passage of a total of 150% of the theoretical charge requirement, d. final appearance of small plates containing pastes C and H. The pastes appeared essentially totally oxidized to β PbO_2. Plates containing oxide C were very dark, nearly black, and plates containing oxide H were lighter in color. The pockets of white material in the lower left quadrant are residual $PbSO_4$ that were not oxidized, possibly because they were not in good electrical contact with the remainder of the pellets. It seems likely that these encrustations would be associated with cracks between the grid metal and paste visible in the radiographs of Fig. 1.

crystals appeared in the paste that originally contained Pb_3O_4, it seems likely that the PbO_2 particles resulting from chemical reaction with H_2SO_4 acted as growth-promoting nuclei. Despite these differences, it would not be possible to identify any single, isolated crystal form as coming from a specific paste, because of the range of individual and agglomerate shapes and sizes in each sample. This is not surprising in view of the fact that all three pastes were primarily composed of the same material after curing, namely tribasic lead sulfate.

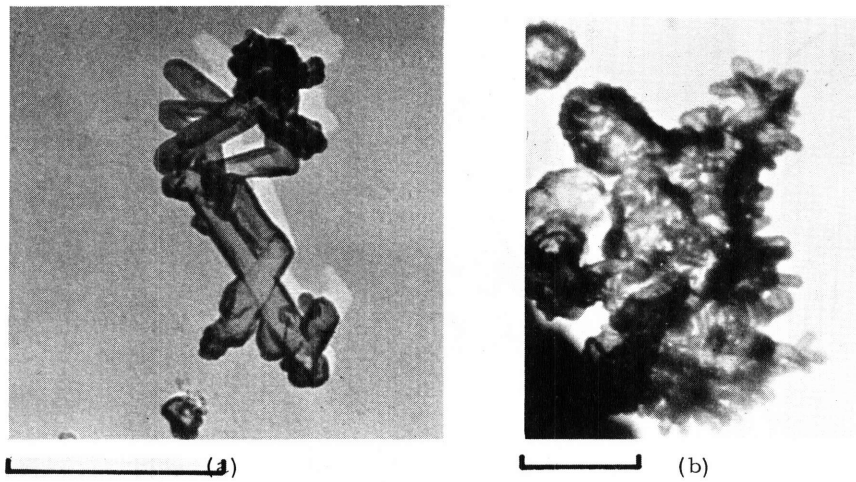

Fig. 4 - Prismatic crystals of PbO_2 (markers equal 1μ). (a) This group of crystals is representative of the type referred to as prismatic individuals with branching suggestive of multiple twinning. They were found more frequently in paste A than in C and H. This is believed to be an early stage in the growth of more extensive clusters of similar prismatic crystals shown in (b) and (b) Christmas-tree dendrites of PbO_2, possibly composed of true whiskers. This may be a more advanced stage of growth of crystal clusters such as shown in (a).

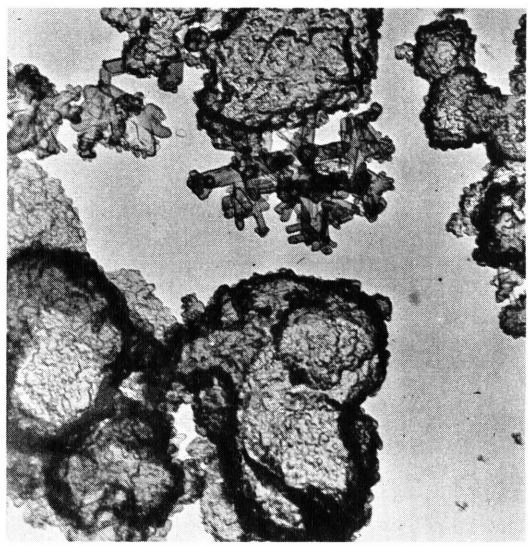

Fig. 5 - Spherulites and prismatic crystals which were characteristic of PbO_2 grown from paste A. It is possible that the spherulites originated from dendrites such as shown here and in Fig. 4 through development of over growths of sessile crystallites on the originally smooth surfaces of the whiskerlike crystals. Marker equals 1μ.

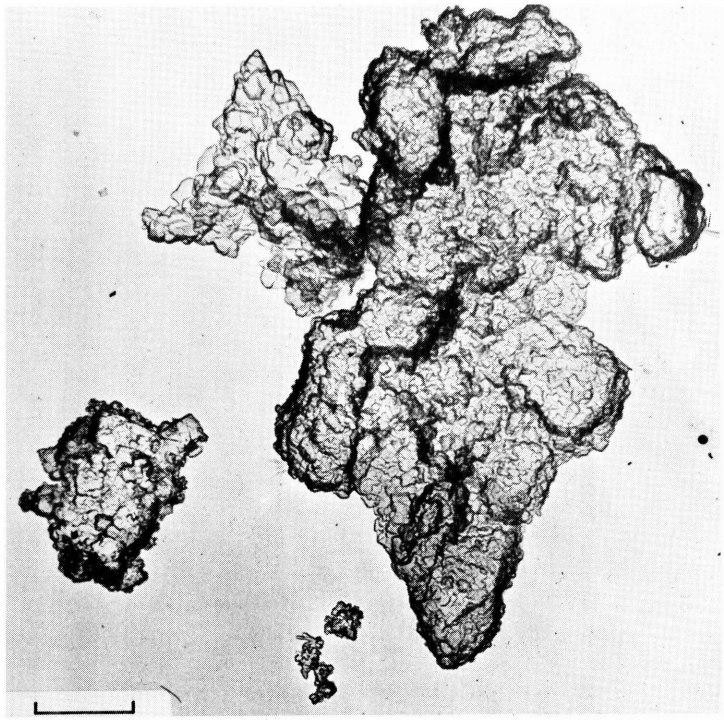

(b)

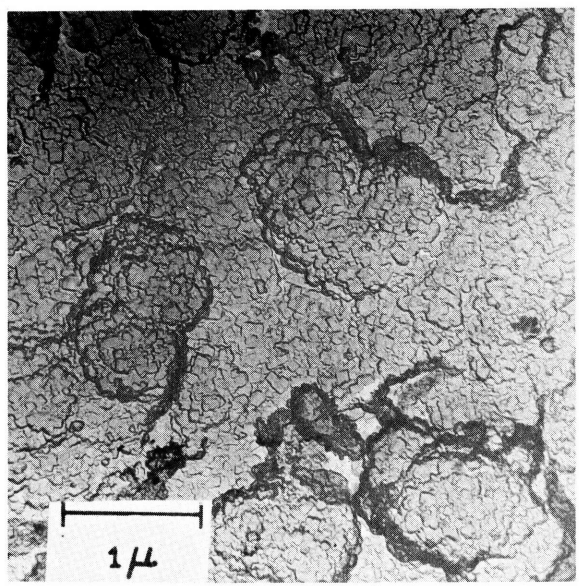

(c)

Fig. 6 - Spheroidal and dendritic growths fairly typical of PbO_2 from paste C. (a) Markers equal 1μ. The similarity in general outline of the emergent dendritic spike to the main body of this nodular mass of crystals is strongly suggestive that the smaller cyrstals have grown on and filled in a similar, underlying dendritic growth of the larger crystals. This is also suggested by the appearance of the smaller mass at the left, which shows a spherulite of larger crystals partially coated with outgrowths of the smaller cyrstals. (b) Detail of a dendritic spike. (c) Spiraling layers of small prismatic crystals make up the spherical nodules. The uniformity in size of these crystallites indicates that they represent one stage in the PbO_2 growth mechanisms, possibly the final stage.

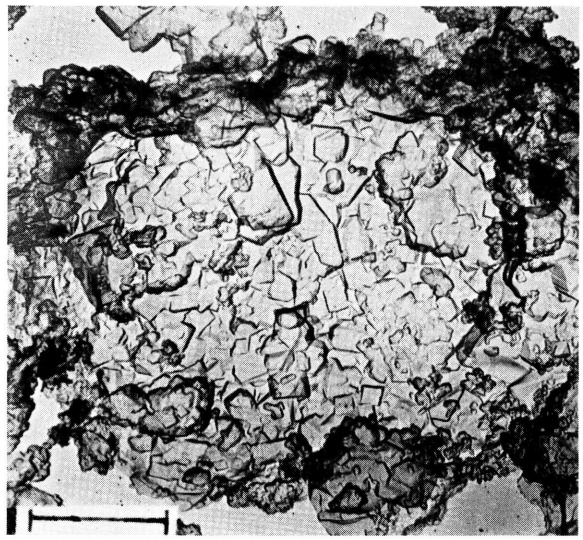

Fig. 7 - Clusters of large prismatic crystals which were characteristic of PbO_2 grown in paste H. The clusters took the form of irregular aggregates, some approaching ovoids and others, like this one, were rhomboidal in outline. The decoration at the edges with much smaller crystallites was also fairly typical and again suggests that the small crystals grow on the surfaces of the larger ones and may represent a final growth stage in the anodic oxidation. Marker equals 1μ.

It did not appear to make a major significant difference in morphology if the paste were formed on the pure lead or antimonial lead grids. This is in contrast to previous observations (4); however, in the earlier study formation was performed by commerical manufacture under considerably different conditions.

ACKNOWLEDGMENT

Appreciation is extended to E.J. Ritchie of Eagle-Picher Industries, Inc., Joplin, Mo., working under a research contract with International Lead Zinc Research Organization, who provided the cured plates used in this study. This contribution included the analyses and characterizations of the oxides, pastes, and metals. Without this cooperative effort this phase of the study would have been impossible.

REFERENCES

1. Burbank, J., and Wales, C.P., "The Lead Calcium Battery, Part 3 - Submarine Cells," NRL Report 5773, May 29, 1962

2. Burbank, J., in "Batteries," D.H. Collins, ed., New York:Pergamon, p. 43, 1963

3. Burbank, J., J. Electrochem. Soc. 111:765 (1964)

4. Burbank, J., J. Electrochem. Soc. 111:1112 (1964)

5. Burbank, J., J. Electrochem. Soc. 113:10 (1966)

6. Burbank, J., in "Power Sources 1966," D.H. Collins, ed., New York:Pergamon, p. 147, 1967

7. Burbank, J., and Wales, C.P., J. Electrochem. Soc. 111:1002 (1964)

8. "Powder Diffraction File," Philadelphia:Am. Soc. Testing Mater.

9. Cowley, J.M., Acta Cryst. 9:391 (1956)

10. Todd, G., and Parry, E., Nature 202:386 (1964)

11. Bode, H., and Voss, E., Electrochim. Acta 1:318 (1959)

12. Ikari, S., Yoshizawa, S., and Okada, S., J. Electrochem. Soc. Japan, Overseas Ed. 27:E 186 (1959)

Security Classification

DOCUMENT CONTROL DATA - R & D

(Security classification of title, body of abstract and indexing annotation must be entered when the overall report is classified)

1. ORIGINATING ACTIVITY *(Corporate author)* Naval Research Laboratory Washington, D.C. 20390	2a. REPORT SECURITY CLASSIFICATION Unclassified 2b. GROUP

3. REPORT TITLE

THE PLATE MATERIALS OF THE LEAD-ACID CELL; PART 4 - ANODIC OXIDATION OF THREE REPRESENTATIVE OXIDES

4. DESCRIPTIVE NOTES *(Type of report and inclusive dates)*

Final report on one phase of the problem; work is continuing on other phases.

5. AUTHOR(S) *(First name, middle initial, last name)*

Jeanne Burbank

6. REPORT DATE September 25, 1968	7a. TOTAL NO. OF PAGES 15	7b. NO. OF REFS 12
8a. CONTRACT OR GRANT NO. NRL Problem C05-14 b. PROJECT NO. SF 013-06-03-4366 c. RR 001-01-43-4755 d.	9a. ORIGINATOR'S REPORT NUMBER(S) NRL Report 6768 9b. OTHER REPORT NO(S) *(Any other numbers that may be assigned this report)*	

10. DISTRIBUTION STATEMENT

This document has been approved for public release and sale; its distribution is unlimited.

11. SUPPLEMENTARY NOTES	12. SPONSORING MILITARY ACTIVITY Department of the Navy (Office of Naval Research and Naval Ship Systems Command), Washington, D.C. 20360

13. ABSTRACT

Three representative lead oxides, designated A, C, and H, for storage-battery fabrication were mixed with water and H_2SO_4 to paste consistency. Each of these was hand pasted into antimonial and pure-lead circular grids of standard SLI thickness. The plates were cured according to common practice for each oxide. The small circular plates were anodized in an electrolytic cell mounted directly on an x-ray machine, and the diffraction patterns were recorded at intervals throughout 72 hr of formation in 1.0585 sp gr H_2SO_4.

X-ray diffraction patterns from the unformed pastes showed the major component was tribasic lead sulfate in all three. The surfaces of plates made from oxides A and H were primarily basic lead carbonate (hydrocerussite), and the surfaces of plates made with oxide C were largely tribasic lead sulfate. Residual PbO and, in the case of oxide H, Pb_3O_4 also were detected. During the soaking period, normal $PbSO_4$ formed on the surfaces of all plates, rapidly eliminating any basic carbonate. During this period Pb_3O_4 in paste H became converted to PbO_2 and $PbSO_4$ causing a marked color change in this kind of plate. As oxidation progressed, dark brown to black βPbO_2 developed near the grid bars and spread gradually toward the pellet centers. Paste A formed at the edges and interior of the pellets but retained a surface coating of $PbSO_4$ at the pellet centers. Pastes C and H appeared essentially completely oxidized, paste C giving a very dark blackish plate, while paste H was lighter in color.

—continues

DD FORM 1 NOV 65 1473 (PAGE 1)

S/N 0101-807-6801

Security Classification

14. KEY WORDS	LINK A ROLE	LINK A WT	LINK B ROLE	LINK B WT	LINK C ROLE	LINK C WT
Lead-acid cells						
Electron morphology						
Oxidation						
Positive plate oxides						
Storage batteries						
Battery paste						
Battery plate formation						
X-ray diffraction						

On completion of anodization, nominally 150% of the theoretical requirement on a weight basis, the pastes were blotted and dried in air at room temperature. The formed paste was removed from the grids for electron-microscope examination by carbon replication. The PbO_2 had a range of morphologies, and the individual crystallites varied from about 0.5 μ to less than 0.1 μ. Some prismatic crystals with branching suggestive of multiple twinning were present in past A and appeared less frequently in the other two pastes. Agglomerates, several microns in size, of prismatic crystallites were present in all pastes. Paste H gave rise to the largest individual crystallites which were about 0.5 μ in diameter. Oxide C resulted in remarkably uniform 0.1-μ crystallites arranged in spiraling layers terminating in one central individual crystallite, forming spheroidal agglomerates. Although not always clearly obvious in the electron micrographs, it is believed that the aggregates are compound spikes of dendritic growth covered with sessile crystallites of varied size and morphology.